Eur Biophys J (1999) 28: 447–456

ARTICLE

Alessandro Paciaroni · Maria Elena Stroppolo
Caterina Arcangeli · Anna Rita Bizzarri
Alessandro Desideri · Salvatore Cannistraro

Incoherent neutron scattering of copper azurin: a comparison with molecular dynamics simulation results

Received: 12 October 1998 / Revised version: 19 February 1999 / Accepted: 1 March 1999

Abstract The low-frequency dynamics of copper azurin has been studied at different temperatures for a dry and deuterium hydrated sample by incoherent neutron scattering and the experimental results have been compared with molecular dynamics (MD) simulations carried out in the same temperature range. Experimental Debye-Waller factors are consistent with a dynamical transition at approximately 200 K which appears partially suppressed in the dry sample. Inelastic and quasielastic scattering indicate that hydration water modulates both vibrational and diffusive motions. The low-temperature experimental dynamical structure factor of the hydrated protein shows an excess of inelastic scattering peaking at about 3 meV and whose position is slightly shifted downwards in the dry sample. Such an excess is reminiscent of the "boson peak" observed in glass-like materials. This vibrational peak is quite well reproduced by MD simulations, although at a lower energy. The experimental quasielastic scattering of the two samples at 300 K shows a two-step relaxation behaviour with similar characteristic times, while the corresponding intensities differ only by a scale factor. Also, MD simulations confirm the two-step diffusive trend, but the slow process seems to be characterized by a decay faster than the experimental one. Comparison with incoherent neutron scattering studies carried out on proteins having different structure indicates that globular proteins display common elastic, quasielastic and inelastic features, with an almost similar hydration dependence, irrespective of their secondary and tertiary structure.

Key words Protein dynamics · Hydration water · Glassy dynamics · Boson peak

A. Paciaroni · A.R. Bizzarri · S. Cannistraro (✉)
Unitá INFM, Dipartimento di Fisica dell'Universitá,
I-06100 Perugia, Italy
e-mail: cannistraro@pg.infn.it

C. Arcangeli · A.R. Bizzarri · S. Cannistraro
Dipartimento Scienze Ambientali, Universitá della Tuscia,
I-01100 Viterbo, Italy

M.E. Stroppolo · A. Desideri
Unitá INFM, Dipartimento di Biologia,
Universitá Tor Vergata, I-00133 Roma, Italy

Introduction

Biological macromolecules, such as nucleic acids and proteins, display a very complex structure which is reflected in a huge variety of breathing and wiggling motions, some of which play an essential role in determining functional properties. Several techniques such as X-ray diffraction, Mössbauer, optical and magnetic resonance spectroscopies, and incoherent neutron scattering (INS), preferentially at different temperatures, have been applied to obtain an appropriate description of the dynamical behaviour of proteins, each technique providing information within different spatial and temporal windows. INS is one of the most powerful approaches since it allows one to investigate atomic dynamics in the pico- and nanosecond time scales, over lengths in the 0.1–100 Å region, probing both vibrational and diffusive motions. Actually, INS from hydrated proteins, such as myoglobin (Mb) (Doster et al. 1989), bacteriorhodopsin (Br) (Ferrand et al. 1993; Fitter et al. 1997) and superoxide dismutase (Sod) (Andreani et al. 1995) pointed out the occurrence of a dynamical transition when the temperature increases above 180–220 K. Below this temperature, the elastic intensity indicated that the protein molecules behave as a harmonic solid, while above it a marked increase in the hydrogen atoms mean square displacements (MSD) suggested the onset of anharmonic motions that have been connected to the activation of transitions among different conformational substates of the polypeptidic chain (Frauenfelder et al. 1988). A similar behaviour has also been observed in some glass-forming systems, such as chain polymers (Frick and Richter 1993, 1995), where

it has been analysed in the framework of the mode-coupling theory (MCT) (Goetze and Sjögren 1992). In this connection, it should be noted that the quasielastic INS intensity of hydrated proteins rises just in correspondence to the dynamical transition and shows a two-step relaxation behaviour, which has been interpreted in terms of fast local (β) and slow collective (α) motions also predicted by the MCT (Doster et al. 1989). Quasielastic scattering has been studied with model dynamical structure factors as well, to take into account the different kind of diffusive atomic motions (Middendorf 1984; Fitter et al. 1997).

The inelastic INS low-temperature spectra of proteins, moreover, have been shown to be characterized by a vibrational peak centred in the range 2–3.5 meV (Cusack and Doster 1990; Smith et al. 1990; Martel et al. 1991; Ferrand et al. 1993; Diehl et al. 1997). The origin of such an excess of scattering, revealed also by Raman scattering (Brown et al. 1972; Genzel et al. 1976; Painter et al. 1982), is not yet well understood. In the past, the protein low-frequency spectrum has been interpreted as the superposition of the vibrational contributions of an elastic sphere (Go 1978), whose characteristic frequencies should be inversely proportional to the radius of the sphere; such a dependence, however, has not been observed (Painter et al. 1982). On the other hand, the modes corresponding to the vibrational peak have been interpreted in terms of accordion-like modes of α-helices (Chou 1985) and their frequencies have been calculated for several proteins in the range 2.5–3.5 meV. By this approach, however, it is not trivial to consider the effects of the solvent. Recently, it has been proposed that the inelastic peak could be related to the dynamics of the hydration water through the librations of the protein side-chains (Diehl et al. 1997). On the other hand, this spectral feature is also reminiscent of the so-called ''boson peak'' observed in the INS and Raman spectra of amorphous disordered materials (Foley et al. 1995; Frick and Richter 1995).

It should be remarked that the general spectral protein features seem to be strictly connected to the solvent properties, e.g. the hydration water dynamics has been hypothesized to be coupled to the dynamics of the protein polar side chains through the injection into the latter of fast excitations which could, in turn, trigger more extensive collective motions of the protein (Fan et al. 1994; Green et al. 1994; Diehl et al. 1997). The dynamical coupling between the hydration water and the protein has been stressed both with several experimental techniques (Doster et al. 1986; Iben et al. 1989; Settles and Doster 1996; Demmel et al. 1997) and with MD simulations (Levitt and Sharon 1988; Steinbach et al. 1991; Bizzarri and Cannistraro 1996; Bizzarri et al. 1996; Steinbach and Brooks 1996; Rocchi et al. 1998). In this respect, MD simulations are a valuable complement to experiments, providing a description of both the protein and the surrounding water at microscopic resolution. Such an approach is particularly rewarding when used in conjunction with INS since both techniques probe the dynamical properties of a protein in the same time window. MD simulations can then be applied to estimate the INS intensities from the calculated atomic trajectories, allowing one to make a direct comparison between experimental and simulated results. In particular, the combination of INS experiments and MD simulation studies has been exploited in the case of Mb, a whole α-helix protein, and contributed to elucidate some interesting aspects, such as the interaction between the protein and the hydration water (Steinbach et al. 1991; Lounnas et al. 1994; Steinbach and Brooks 1996) and the determination of the protein internal motions (Smith et al. 1989; Smith and Kneller 1993). In recent years, some of the authors have been involved in a systematic investigation of the dynamics of copper containing proteins characterized by a β-barrel structural folding such as the dimeric Sod and the monomeric plastocyanin (Pc) through both an experimental (Andreani et al. 1995) and a simulative approach (Melchionna et al. 1988; Bizzarri and Cannistraro 1996; Arcangeli et al. 1998; Rocchi et al. 1998). In an effort to extend such a study and on the basis of previous MD simulations results, which pointed out the presence of a broad low-frequency inelastic peak just in the Pc hydration water (Paciaroni et al. 1998), an INS investigation of azurin (Az), a copper containing β-barrel protein characterized by a 3D structure similar to Pc, has been performed, with the aim at better understanding the low-frequency dynamical behaviour of the water-protein system.

In this work the preliminary results of such research, mainly concerning the dynamical features of hydrated Az, are reported. Two samples, one deuterium hydrated and the other almost dry, have been studied at four different temperatures. MD simulations at the same temperature values have been carried out as well.

Elastic, quasielastic and inelastic features of Az are found to be similar to those of other proteins possessing different structures, and display almost the same hydration dependence. These features find correspondence in glass-forming materials, especially concerning the low-frequency vibrational behaviour, which is mainly characterized by an excess of inelastic scattering at about 3 meV. MD simulations reproduce quite well the INS spectral behaviour of the hydrated protein as a function of the temperature.

Materials and methods

Preparation of the samples

The Az gene from *Pseudomonas aeruginosa* was cloned from pSE420 (Invitrogen) and heterologously expressed in *Escherichia coli* 7118 strain (Messing et al. 1977). Recombinant *E. coli* clones were grown in standard LB medium containing ampicillin (50 mg/ml) for 8 h at 210 K. The protein was purified from the periplasmic fraction through a FPLC apparatus equipped with a

HiLoad 16/60 Superdex 75 column (Pharmacia) and eluted as a single peak. The procedure was repeated to obtain a protein purity grade higher than 98%, as judged by SDS-PAGE electrophoresis. Az, which has a molecular weight of 14 kDa, was lyophilized to obtain a light blue powder and then dehydrated in a chamber in the presence of P_2O_5, under vacuum, for 2 days. Hydration of azurin at 0.36 g D_2O/g protein was carried out by controlled hydration in a chamber under vacuum in the presence of a saturated KCl deuterium solution. The water content was settled by measuring the increase in weight of the protein sample. An almost dry sample was obtained from a H_2O hydrated sample which was dried to below $h = 0.13$ g H_2O/g protein.

Incoherent neutron scattering

Measurements were made on the cold neutron multichopper time-of-flight spectrometer IN5 at the Institut Laue Langevin (ILL). Time-of-flight is a general method for finding the energy of a neutron by measuring the time t_F it takes to fly between two points (Bèe 1988). By measuring the number of neutrons that arrive after t_F in the detector acceptance area Ω corresponding to the scattering angle 2θ, one reveals the time-of-flight cross section, $\partial^2\sigma(2\theta,t_F)/\partial\Omega\partial t_F$. From such a quantity it is possible to derive the so-called dynamical structure factor $S(2\theta,v)$ as a function of the exchanged energy hv (Bèe 1988), provided that both the distance between sample and detectors and the incident energy are known. The dynamical structure factor at a fixed exchanged momentum $\hbar q$ value $S(q,v)$ can be derived from $S(2\theta,v)$ by interpolation of the experimental data, taking into account the kinematical law that involves q and 2θ (Bèe 1988). Actually, the data were taken with an incident wavelength of $\lambda = 6$-Å, resulting in an elastic resolution of about 60 μeV (full width at half height at the elastic peak), a range of q from 0.4 to 1.8 $Å^{-1}$, and an accessible energy range from approximately −1.5 meV up to $2K_BT$ (from energy loss to energy gain domain). The data were corrected using standard ILL programs to take into account incident flux, cell scattering, self shielding and detector response, referring to a vanadium standard. The 81 spectra recorded have been binned into 12 groups to improve the counting statistics. An average transmission of 92% was obtained. Therefore multiple scattering or multiphonon corrections were not applied.

Spectra were accumulated for 6–8 h at the temperatures $T = 100$, 180, 220 and 300 K for the hydrated sample and for 3–5 h at the temperatures 180 and 300 K for the dry sample. In any case, an amount of 300–350 mg of sample was held in a standard flat aluminum cell with internal spacing 1.5 mm, placed at an angle of 135° to the incident beam.

The incoherent scattering intensity is usually separated into an elastic, a quasielastic and an inelastic part. Actually, in the one-phonon scattering approximation (Lovesey 1986), taking into account only the contribution of the hydrogen atoms which have a strong incoherent cross section, the following relationship holds:

$$S(q,v) = \mathrm{DWF}(T)[\mathrm{EISF}(q)\delta(v) + (1 - \mathrm{EISF}(q))S_{\mathrm{qel}}(q,v)] + \mathrm{DWF}(T)\frac{q^2}{8\pi M v}n(v,T)g(v) \quad (1)$$

where EISF(q) is the elastic incoherent structure factor. The first term represents the elastic scattering, which gives information on the geometry of the volume accessible to the sample atoms at infinite time (Lovesey 1986). Elastic scattering dependence on the energy is represented as a delta function and the Debye-Waller factor is:

$$\mathrm{DWF}(T) = \exp\{-q^2\langle u^2(T)\rangle/3\} \quad (2)$$

where $\langle u^2(T)\rangle$ are the averaged hydrogen MSD. Equation 2 can be applied to estimate the atomic MSD through a fit of the elastic line. The quasielastic part $S_{\mathrm{qel}}(q,v)$ represents the broadening of the elastic peak and indicates the presence of non-vibrational, diffusive motions in the sample. The last term, describing the inelastic contribution, results from exchange of energy with vibrational modes in the molecule; M is the proton mass, $g(v)$ is the vibrational density of states, and $n(v,T) = (\exp(hv/k_BT) - 1)^{-1}$ is the Bose factor. Actually, in the measured spectra, all the terms in Eq. 1 are convoluted with the experimental resolution.

MD simulation methods

Initial coordinates of oxidized Az from *P. aeruginosa* were taken from the second segment of the tetramer comprising the X-ray crystal structure at 1.93 Å resolution (4AZU entry of Brookhaven Protein Data Bank) (Nar et al. 1991). The MD trajectories of Az were generated by an integration step of 0.002 ps using the GROMOS96 program package (van Gunsteren and Berendsen 1996) including the SPC/E potential for water (Berendsen et al. 1987). The disulfide bridge between the cysteine residues 3 and 26 has been introduced.

To treat the copper site, according to the recent approach used for Pc (Ciocchetti et al. 1997; Ungar et al. 1997), a covalent bond between the copper and each of the five ligands was introduced to preserve the X-ray structure. In particular, the copper ion of Az was coordinated to two side chain nitrogens (His46 and His117), to two side chain sulfurs (Cys112 and Met121) and to a carbonyl oxygen (Gly45) to give a distorted trigonal bipyramidal geometry. All the ionizable residues, with the exception of those providing the copper ligands, have been assumed to be in the ionization state derived according to the pH value of 5.5 of the crystal. The charge of Cys112 was set to −0.5e, while His46, His117, Met1121 and Gly45 are considered neutral; a charge of 0.5e was given to the copper ion. The resulting total protein charge is then −3e.

The Az system at the required hydration level of $h = 0.40$ g of H_2O/g of protein was derived from the fully hydrated system, equilibrated at 300 K for 150 ps, obtained by an Az molecule centred in a truncated octahedron from a cube of edge 63.4998 Å filled with 3600 bulk SPC/E waters. In particular, 315 waters were extracted by removing any water molecules at a distance greater than 3.31 Å from any protein atom, a minimum distance of 2.3 Å between the waters and the protein atoms having been imposed. MD simulations of Az hydrated at $h = 0.40$ g D_2O/g of protein were obtained by replacement of water hydrogens with deuterium.

Cutoff radii of 8 Å for the non-bonded interactions and of 14 Å for the long-range charged interactions were used, respectively. Two hundred steps of energy minimization with the steepest descent method, in the presence of a harmonic position restraining force with a constant equal to 90 kJ/mol per Å^2, were performed.

MD trajectories of D_2O hydrated Az were followed for 600 ps at different temperature: $T = 100$, 180, 220 and 300 K. Simulations at the various temperatures were performed by first assigning, to each atom, Maxwellian velocities at 20, 40 and 50 K, and progressively increasing the temperature during the first 20 ps. The temperature of the protein and of the solvent was separately coupled to an external bath with relaxation times progressively increasing from 0.01 ps to 0.1 ps during the first 20 ps. A decreasing positional restraining force, with a constant going from 50 kJ/mol per Å^2 to 5 kJ/mol per Å^2 was also applied during the first 20 ps. Any residual translational and rotational motion of the centre of mass was removed from the initial velocities. Configurations of all trajectories and energy were saved every 0.01 or 0.1 ps. The neighbour pair list was updated every 10 steps. The Shake constraint algorithm (Ryckaert et al. 1977) was used throughout the simulation to fix the internal geometry of the water molecules and to keep bond lengths of the protein rigorously fixed at their equilibrium values.

On the basis of the monitoring over the kinetic and potential energy, the root mean square deviation of the Az backbone and the gyration radius, it comes out that all the systems have reached thermal equilibrium within the first 100 ps. After such an initial period used to equilibrate the system, a 500 ps production run was performed.

A measure of the protein motions' extent is provided by the calculation of the atomic MSD, which are directly comparable with the corresponding experimental values obtained from the Debye-Waller factor. In fact, the MSD of ith atom can be derived from the MD trajectories through the relationship:

$$u_i^2 = \frac{1}{3}\left\langle (\Delta x_i)^2 + (\Delta y_i)^2 + (\Delta z_i)^2 \right\rangle \tag{3}$$

where x_i, y_i and z_i are the differences between the instantaneous and averaged coordinates of the ith atom and the brackets $\langle\ \rangle$ represent a time average.

To compare the MD results with the experimental ones, the stored trajectories of the non-exchangeable hydrogen atoms of the protein (approximately the 80% of the total) were exploited to calculate the self intermediate scattering function $I(\boldsymbol{q},t)$; such a function, which is the incoherent part of the total intermediate scattering function describing the dynamics of the spatial Fourier components of particle density fluctuations of wave vector $\boldsymbol{q}$, can be derived through:

$$I(q,t) = 1/3N\left\langle \sum_{i=1}^{N} \exp[i\boldsymbol{q}\cdot(\boldsymbol{R}_i(t) - \boldsymbol{R}_i(0))] \right\rangle \tag{4}$$

where $\boldsymbol{R}_i(t)$ is the position vector of the ith atom at time t, and the brackets $\langle\ \rangle$ denote an averaging over both the protein ensemble and the exchanged momenta $\boldsymbol{q}$ having the same modulus q, to take into account anisotropic effects. The incoherent dynamical structure factor $S(q,v)$ can be directly calculated by the time Fourier transform of $I(\boldsymbol{q},t)$:

$$S(q,v) = \frac{1}{2\pi}\int_{-\infty}^{+\infty} \mathrm{d}t \exp\{(-2i\pi vt)\} I(q,t) \tag{5}$$

In applying Eq. 5, a numerical fast Fourier transform was used, and the calculated $S(q,v)$ was convoluted with a function describing the real experimental resolution function.

In order to calculate a dynamical structure factor satisfying the detailed balance condition, which is usually not verified when the $S(q,v)$ is calculated with Eq. 5, a semiclassical correction was applied by multiplying $S(q,v)$ by the factor $\exp(hv/2k_BT)$ (Kneller et al. 1995).

The vibrational density of states $g(v)$ was derived from the spectral density $C_{vv}(v)$ of the velocity autocorrelation function $C_{vv}(t)$ (Paciaroni et al. 1998), calculated for all the protein hydrogens:

$$g(v) \sim C_{vv}(v) = \frac{1}{2\pi}\int_{-\infty}^{\infty} \mathrm{d}t \exp(-2i\pi vt) C_{vv}(t) \tag{6}$$

where $C_{vv}(t)$ was obtained by considering only the non-exchangeable hydrogen atoms which provide the largest contribution to $g(v)$. In addition, $C_{vv}(t)$ has been multiplied by a gaussian damping envelope to overcome spurious truncation effects and a spherical average has been applied to take into account anisotropic effects (Kneller et al. 1995).

Results and discussion

The dynamical structure factor $S(2\theta,v)$ of hydrated Az, which contains information about the sample structure and dynamics, is dominated by the incoherent contribution of the protein protons; such a quantity is shown in Fig. 1 as a function of energy at a fixed scattering

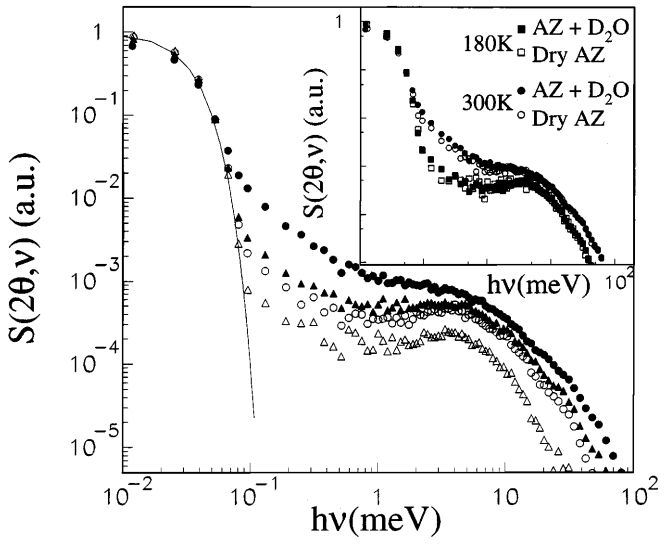

Fig. 1 Measured $S(2\theta,\nu)$ of Az sample hydrated at 0.36 g D_2O/g protein and at $2\theta = 105°$ as a function of the temperature: 100 K (*open triangles*), 180 K (*open circles*), 220 K (*solid triangles*) and 300 K (*solid circles*). The same symbols will be used for the following figures. *Inset*: comparison between spectra of D_2O hydrated Az (*solid symbols*) and dry Az (*open symbols*) at 180 K (*squares*) and 300 K (*circles*)

angle $2\theta = 105°$ and at the four measured temperatures. Each spectrum may be considered as the sum of three different contributions, i.e. the elastic, quasielastic and inelastic as described in the Materials and methods section. As can be seen in Fig. 1, the elastic peak is not a delta function but has a well-defined linewidth, because of the finite experimental resolution (represented with the full line in the figure), such a linewidth corresponding to the limit of the slowest observable motions. The elastic intensity decreases upon increasing the temperature, according to the Debye-Waller factor behaviour (see Eq. 2), and such a decrease is compensated for by quasielastic and inelastic scattering.

In the Debye approximation, the low-frequency dependence of the vibrational density of states ($\sim\nu^2$) is cancelled by the two factors $n(\nu,T) \sim k_B T/\nu$ and $1/\nu$; therefore the inelastic term that appears in Eq. 1 should contribute as a constant to $S(q,\nu)$. Indeed, the low-frequency inelastic spectra show a well-defined excess intensity around 3 meV over the simple Debye-like behaviour, particularly visible at low temperatures. As the temperature increases, such a peak becomes less distinguishable, owing to the rise of the quasielastic contribution which gradually fills up the low-temperature minimum. A quite similar behaviour is exhibited by the INS spectra of the dry sample at 180 K and 300 K; these are shown in the inset of Fig. 1 together with the spectra from the corresponding hydrated sample. At 180 K a slight downwards shift of the inelastic peak is observed in the dry sample, with respect to the hydrated one (this point is better emphasized below), while at room temperature the quasielastic contribution of the dry sample is slightly lower than the hydrated one; such behaviour in the quasielastic intensity has been revealed more clearly also in other proteins (Diehl et al. 1997) where, in addition, the dry sample exhibits an inelastic scattering centred at about 2 meV which is more intense than that of the hydrated one.

The decrease of the elastic intensity as a function of the temperature observed in Fig. 1 is related to an increase of the atomic mobility, as appears from the Debye-Waller factor represented by Eq. 2. The protein hydrogen MSD have been obtained by fitting the elastic intensity in the q range from 0.4 $Å^{-1}$ to 1 $Å^{-1}$ at the four experimental temperatures. Even though in the present study the number of experimental points as a function of the temperature is much smaller than in other INS protein investigations, the behaviour of hydrated Az seems to confirm the results obtained for Mb (Doster et al. 1989) and Sod (Andreani et al. 1995) at similar hydration conditions, as shown in Fig. 2. In addition, our experimental MSD data are also consistent with the corresponding data, including the X-ray B-factors (data not shown) as obtained by other techniques (Parak et al. 1982; Nar et al. 1991). The measured MSD point out a harmonic trend until about 200 K, at which point a departure from the low-temperature linear behaviour marks a dynamical transition. The two experimental points available for the dry sample seem to indicate a less marked mobility, in agreement with the results found in partially hydrated Sod (Andreani et al. 1995) and dry Br in purple membrane (Ferrand et al. 1993). Figure 2 shows also the MSD calculated from the non-exchangeable hydrogen atoms trajectories of the MD simulated deuterium-hydrated Az sample. They appear to vary more rapidly than linearly with the temperature, especially above 180 K. In this respect, our MD data

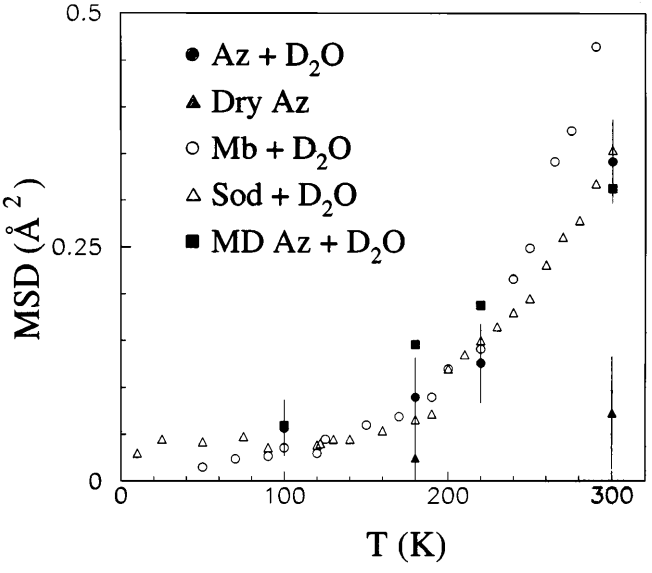

Fig. 2 MSD obtained from the experimental neutron elastic intensity of D_2O hydrated and dry samples and from MD simulations of D_2O hydrated Az (rescaled by a factor of 0.4). For comparison the MSD of other proteins are also displayed

might be consistent with the occurrence of the dynamical transition as observed in the experiments. We note that the MD results have been rescaled by a factor 0.4 in order to show them together with the quite lower experimental points. A similar quantitative discrepancy between the experimental and the MD computed MSD has been already observed in hydrated Mb (Steinbach et al. 1991) where another potential (CHARMM) has been used, and it may originate from a too soft MD force field which could lead to an overestimate of the atomic fluctuations (Parak and Knapp 1984; Paciaroni et al. 1998). In this respect, however, also an effect due to the truncation of the electrostatic interaction could be accounted for.

The noticeable low-temperature inelastic bump revealed in the hydrated Az sample is better emphasized in Fig. 3, where the experimental data are displayed in the $S(q,\nu)$ representation at $q = 1.8$ Å^{-1} for all the four investigated temperatures. In this description, which includes an average over adjacent values of energy as well, the hydrated sample shows a broad low-frequency inelastic band centred around approximately 3 meV, which is well visible up to 220 K, but merges into the quasielastic contribution at room temperature. The inelastic origin of the peak is furtherly supported by the q^2 dependence of its intensity, predicted by Eq. 1, as is shown in the inset of Fig. 3 at $T = 180$ K. Figure 3 shows also the spectra for the dry Az sample (stars) at 180 K and at 300 K. In such a sample the inelastic peak can be seen as well at 180 K, but peaking at about 2.5 meV, slightly downwards shifted with respect to the corresponding hydrated sample; such an effect is in agreement with the results found in a recent INS investigation of dry and hydrated Mb and lysozyme (Lys) (Diehl et al. 1997). The presence of an excess of scattering quite similar to that shown in Fig. 3, located in approximately the same range of 2–3.5 meV, has been seen in the low-temperature INS spectra of several proteins at different hydration conditions, such as Mb (Smith et al. 1989; Cusack and Doster 1990; Doster et al. 1990), Lys (Cusack and Doster 1990; Diehl et al. 1997), bovine pancreatic trypsin inhibitor (Cusack 1989; Cusack and Doster 1990), hemoglobin and red blood cells (Martel et al. 1991) and Br in purple membrane (Ferrand et al. 1993). Such a peak, whose attribution has been discussed in the Introduction, was also revealed by Raman scattering in several proteins at room temperature (Brown et al. 1972; Genzel et al. 1976; Painter et al. 1982). In addition, an excess of scattering at the same position has been observed in INS spectra of both heat and acid denatured Mb (Cusack and Doster 1990) and a mixture of hydrated amino acids (Diehl et al. 1997), indicating that the vibrations corresponding to the peak are independent of the main-chain conformation and packing and of the monomer chemical linkage (Cusack and Doster 1990). Such an observed independence has lead some authors to indicate that the side chains in the protein are responsible for the dynamical contribution to the low-frequency spectral features (Cusack and Doster 1990), even if such a low-energy bump could be also related to collective motions. This hypothesis, which reconciles the inelastic excess of scattering to the side-chains libration dynamics, seems to be supported by the observed dependence of the peak position on the hydration degree. In fact, the dynamical behaviour of the side chains, in particular near the protein surface, is strongly affected by the interaction with the surrounding water molecules (see also the Introduction).

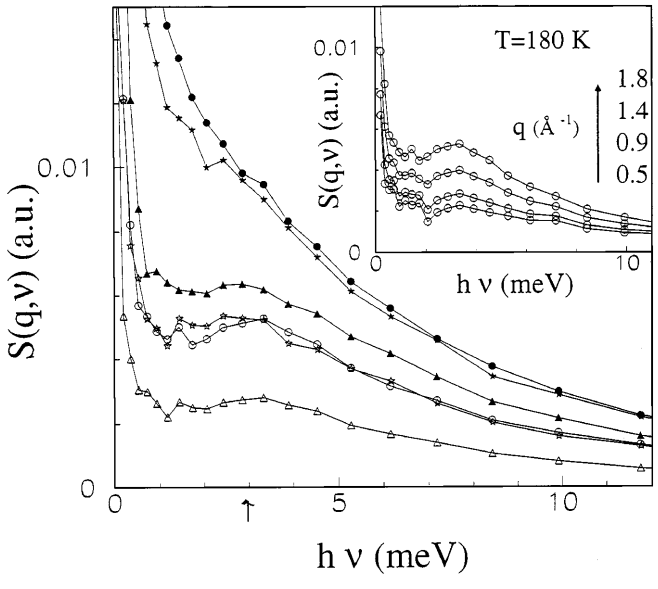

Fig. 3 Experimental incoherent dynamical structure factor of D_2O hydrated and dry Az (*stars*) as a function of temperature at $q = 1.8$ Å^{-1}. *Inset*: experimental incoherent dynamic structure factor of D_2O hydrated Az at $T = 180$ K and at $q = 0.5$, 0.9, 1.4 and 1.8 Å^{-1} *from the bottom to the top*. At low q, the $S(q,\nu)$ at the high energy value has been obtained through an extrapolation, because of the kinematical constraints

On the other hand, it should be remarked that the excess of inelastic scattering observed in proteins is reminiscent of a similar low-frequency inelastic feature revealed in the INS spectra of amorphous disordered materials, where it has been usually called a "boson peak" (Elliott 1992; Frick and Richter 1995). In glass-like systems, the inelastic peak has been observed in a range between 0.1 and 5 meV (Frick and Richter 1995) and its intensity seems to show a q^2 dependence (Frick and Richter 1993). The similarity between proteins and glasses in the inelastic spectral behaviour should not be surprising because the dynamical behaviour of native proteins shows some features that can be related to so-called "glassy" dynamics (Iben et al. 1989; Angell 1995). The protein-glass analogy, by which the dynamics of a single protein macromolecule is interpreted in terms of that of a many-particle glass-forming system, resides mainly in the existence of a huge number of nearly conformational substates, regulating the kinetic response of the protein (Iben et al. 1989) and constituting a potential energy hypersurface similar to that of a

many-particle glass-forming system (Green et al. 1994). Even in the case of some amorphous systems such as the polymers, the chains formed by several simple units have been indicated as being responsible for the low-frequency inelastic spectral behaviour with both correlated motions of neighbouring polymer chains and uncorrelated motions of different polymer chains (Buchenau et al. 1996).

The origin of the boson peak observed in glasses has been often attributed to some topological properties of the system (Elliott 1992), and it has been hypothesized that the vibrations at and below such a peak are localized vibrations, coexisting and interacting with sound waves (Buchenau 1992). It would be interesting to understand how and under which conditions a similar picture can be applied to interpret the dynamical behaviour of proteins. On such a ground, it could be speculated that, as has been supposed for the boson peak of the amorphous materials (Zeller and Pohl 1971; Elliott 1992; Sokolov et al. 1992), the inelastic excess of scattering observed in INS protein spectra might originate from a structural correlation over an intermediate range scale; these structural inhomogeneities, associated with localized excitations, then give rise to a strong scattering of acoustic phonons (Elliott 1992). In the Debye approximation, a relationship between the peak frequency v_0 and the correlation length ξ, characterizing the intermediate-range order, has been postulated (Elliott 1992):

$$v_0 = \frac{v_s}{2\xi} \tag{7}$$

where v_s is the sound velocity. It is not easy to obtain a reliable estimate of the acoustic mode propagation velocity in hydrated protein systems. However, a value for v_s has been suggested, ranging between 2000 and 4000 m/s for proteins at different hydration levels (Doster et al. 1986; Bellissent-Funel et al. 1989). By using such values, together with a boson peak frequency $v_0 \sim 3$ meV, Eq. 7 provides a correlation length ξ between 14 and 28 Å. In this framework, it appears quite questionable to attribute a physical meaning to such a correlation length, especially if one considers that the system under investigation consists of one layer of water molecules in intimate contact with the lateral side-chains of the protein milieu, whose spatial extention spans a region of about 40 Å. It could be, therefore, speculated that the observed vibrational peak could result from the interaction of side-chain units which may also belong to non-neighbour amino acids and give rise to some collective motions.

The MD simulated $S(q,v)$ of hydrated Az, which have been obtained by calculating the Fourier transform of the $I(q,t)$ (see the Materials and methods section), can be seen in Fig. 4 and reproduce qualitatively an inelastic excess of scattering which shows a q^2 dependence (not shown). The inelastic peak, which is a clearly visible up to 220 K, is, however, slightly shifted from 3 meV to about 1.5 meV. The discrepancy between MD simulations and experiments has also been observed in Mb (Smith et al. 1989; Longarich and Brooks 1990; Smith 1991; Steinbach et al. 1991), where the MD simulations were performed using a different potential force field (CHARMM) (Steinbach et al. 1991). Such a downwards shift, which could be another manifestation of a too soft potential force field, or could be related to electrostatic truncation or intermolecular interactions between more than three molecules, may be connected to the overestimate of the MSD, as it occurs in a classical harmonic oscillator, where the amplitude of the fluctuations is inversely proportional to the frequency (Steinbach et al. 1991; Diehl et al. 1997; Paciaroni et al. 1998). The presence of the boson peak in the simulated protein can also be put forward as evidence for an excess of low-frequency modes in $g(v)$ (Frick and Richter 1995). Actually, in the inset of Fig. 4, the ratio $g(v)/v^2$, calculated as described in the Materials and methods section, is shown for various temperatures, revealing the presence of a bump, located at about 1.5 meV for 100, 180 and 220 K. The density of the low-frequency vibrations increases with the temperature and, as a consequence, the maximum of $g(v)/v^2$ is shifting to lower energies, while at 300 K, well above the temperature at which the dynamical transition occurs, a Debye-like behaviour is registered in the low-frequency region. A similar behaviour has been found also in many different glass formers (Wuttke et al. 1995).

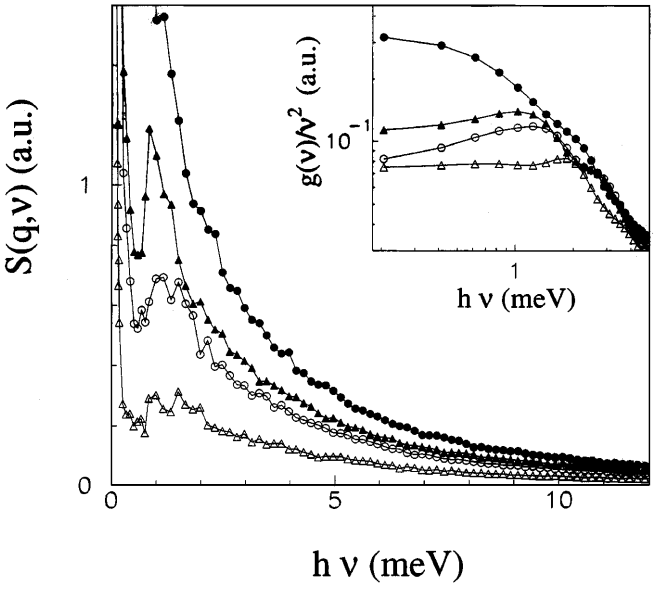

Fig. 4 MD calculated incoherent dynamical structure factor of D_2O hydrated Az for different temperatures, at $q = 1.8$ Å^{-1}. *Inset*: MD calculated vibrational density of states as a function of temperature

Figure 5 shows the INS spectra of hydrated Az after their rescaling by the Bose factor to a common temperature $T = 100$ K. For a perfect harmonic solid, such a scaling should give the same spectrum at all temperatures, within the experimental errors. Superposition of the spectra onto a master curve occurs only at and above the inelastic peak for all the temperatures, suggesting

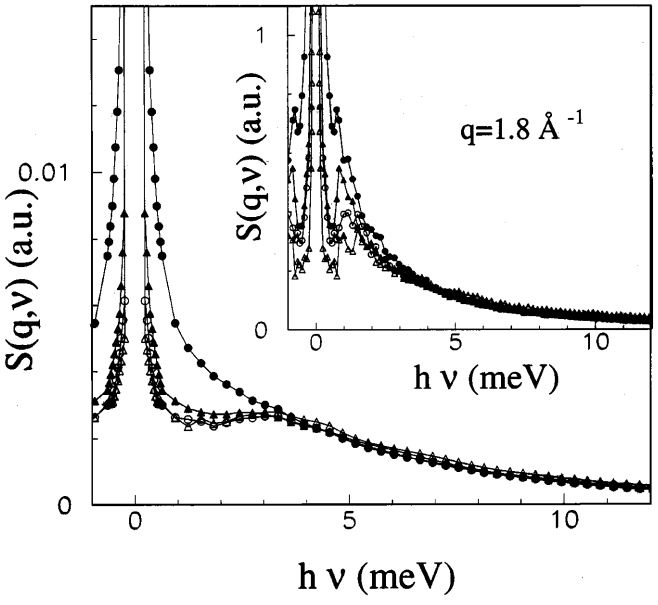

Fig. 5 Experimental incoherent dynamical structure factor of D_2O hydrated Az for different temperatures, at $q = 1.8$ Å^{-1} obtained after rescaling by the Bose factor to a common temperature $T = 100$ K. *Inset*: MD calculated dynamical structure factor after rescaling by the Bose factor

that in this region the vibrations are harmonic (Frick and Richter 1993). The $S(q,v)$ are superimposable, however, for all the energies at 100 K and 180 K, where the elastic peak shows no broadening; at 220 K a little quasielastic scattering contribution appears as a hardly visible broadening of the elastic peak. At 300 K the quasielastic contribution becomes much more intense and the increases in the elastic linewidth reflects the onset of diffusive anharmonic motions. By analogy with the experimental case, the harmonic behaviour has been studied also in the MD semiclassically corrected $S(q,v)$ which have been rescaled by the Bose factor. The spectra, displayed in the inset of Fig. 5, show a harmonic dependence above approximately 2 meV for all the temperatures. In this case, however, the spectra at 100 K and at 180 K are not superimposable and, by increasing the temperature, both the quasielastic and the inelastic scattering rise until 300 K where the first one becomes the main contribution.

The quasielastic scattering, which results from very complex diffusive atomic motions, is quite difficult to analyse. In previous INS studies it was proposed that the various kinds of atomic motion can be represented through an ad hoc $S_{qel}(q,v)$ expressed as the sum of lorentzian contributions, and the experimental data were consequently fitted following such a model (Andreani et al. 1995; Fitter et al. 1997). Such an approach is usually applied in conjunction with a quite good experimental resolution, which is not attained under the experimental conditions in the present work. On such a ground, the quasielastic part has been analysed following a procedure already applied in an INS investigation of Mb (Cusack and Doster 1990; Doster et al. 1990), which is based on the hypothesis that harmonic and anharmonic motions are statistically independent (Cusack and Doster 1990; Doster et al. 1990). In this approach, the quasielastic contribution at temperature T can be estimated by a careful subtraction of the vibrational part from the total spectrum:

$$S^T_{\mathrm{qel}}(q,v) = S^T(q,v) - S^T_{\mathrm{VIB}}(q,v) \tag{8}$$

Because of their harmonic behaviour, low-temperature spectra at T_0 can be used to approximate the vibrational component at higher temperature T, through the relationship (Cusack and Doster 1990):

$$S^T_{\mathrm{VIB}}(q,v) = S^{T_0}(q,v)\mathrm{DWF}(T)n(v,T)/\mathrm{DWF}(T_0)n(v,T_0) \tag{9}$$

Such a procedure has been applied to the experimental $S(q,v)$ of hydrated and dry Az and to the simulated of hydrated Az, using as low-temperature harmonic intensities the spectra at 100, 180 and 100 K. In Fig. 6a the experimental quasielastic contribution is shown for hydrated Az and dry Az at $T = 300$ K. The two samples show the same trend and the corresponding intensities differ only by a scale factor.

According to a MCT based description of the protein dynamical behaviour (Doster et al. 1989, 1990), quasielastic scattering can be interpreted as the superposition of the fast β local motions of particles caged in a heat bath of nearest neighbours and of the slow α collective motions arising from the rearrangement of the cages (Goetze and Sjögren 1992). On such a ground, it has been

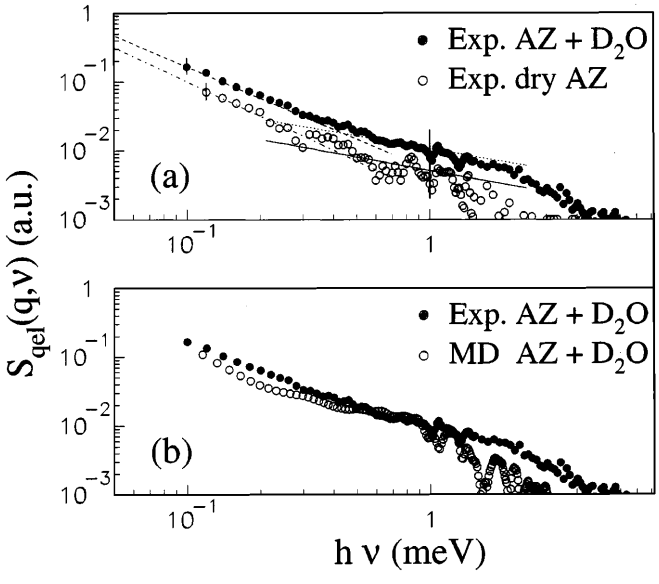

Fig. 6a, b Quasielastic contribution to incoherent neutron scattering. **a** Quasielastic intensities of D_2O hydrated and dry samples are plotted at $q = 1.8$ Å^{-1} and $T = 300$ K together with the result of the fit with the two-power law of Eq. 10. **b** Quasielastic intensities of D_2O hydrated experimental and simulated Az are plotted at $q = 1.8$ Å^{-1} and $T = 300$ K

proposed that the quasielastic contribution can be represented by a model function containing two power law components (Doster et al. 1989, 1990; Diehl et al. 1997) which describes slow and fast dynamical processes:

$$S(q, v) \propto Av^{-1-b} + Bv^{-1+\alpha} \quad (10)$$

It should be noticed that in the case of the Brownian motion of large particles suspended in a solvent composed of many small particles, the two coefficients should be $b = 1$ and $a = 1$, corresponding respectively to the lorentzian function describing the diffusion of the large particles, and to the white noise resulting from the faster dynamics of the solvent. In Fig. 6a are shown also the lines representing the fit of the experimental data with Eq. 10 for the two samples. Even though the calculated values a and b are quite scattered ($a = 0.45 \pm 0.15$, $b = 0.5 \pm 0.15$ for hydrated Az and $a = 0.40 \pm 0.15$, $b = 0.55 \pm 0.15$ for dry Az), it can be observed that the curves corresponding to the two power laws intersect at nearly the same energy (approximately 0.4 meV) in both the samples, indicating that the characteristic times involved in the diffusive motion processes are independent of the hydration. In addition, these values are comparable with those derived for Mb (Doster et al. 1990), a whole α-helix protein, suggesting that globular proteins could have characteristic relaxational times of α and β processes, which are quite similar, irrespective of both their secondary and tertiary structure and their hydration degree. In Fig. 6b the experimental and MD computed quasielastic contribution at room temperature are shown. The simulated scattering agrees quite well with the experimental one, especially between 0.4 meV and 1 meV, while at low energies the two curves display different trends. Since in such a low-energy range the spectra are determined by the slow collective motions, it could be suggested that also this discrepancy could be ascribed to an underestimate of the long-range interatomic potential energy which would soften the dynamics of the mechanisms related to the collective motions.

Conclusions

INS experiments and MD simulations of D_2O hydrated and dry Az have been carried out as a function of the temperature. Elastic, quasielastic and inelastic features of Az are similar to other proteins with different secondary and tertiary structure. In addition, almost the same hydration dependence is exhibited. The MSD derived from experimental Debye-Waller factors and from MD simulations are consistent with a dynamical transition at approximately 200 K. In both the hydrated and dry sample the quasielastic INS at 300 K is characterized by a two-step relaxation behaviour and the corresponding intensities differ only by a scale factor, showing similar characteristic relaxational times. Experimental spectra of the hydrated sample at low temperatures show the presence of a vibrational peak around 3 meV. Such an inelastic excess of scattering, which seems to originate from harmonic vibrations, is reminiscent of the boson peak observed in amorphous disordered materials. The MD simulation reproduces quite well the inelastic bump, but with quantitative differences concerning its position. The discrepancies observed between the experimental and MD calculated INS spectra can be attributed to different effects related to a too soft potential force field, or to electrostatic truncation. It is interesting to remark that a potential force field able to reproduce the INS results could entitle one to exploit MD simulations to investigate, at an atomic level, the nature of the dynamical processes related to the inelastic peak. In this connection, the vibrational motions corresponding to such a peak could be analysed in detail, for example by screening the spectral contribution from every single protein atom.

Acknowledgements We thank ILL for providing neutron facilities.

References

Andreani C, Filabozzi A, Menzinger F, Desideri A, Deriu A, Di Cola D (1995) Dynamics of hydrogen atoms in superoxide dismutase by quasielastic neutron scattering. Biophys J 68: 2519–2523

Angell CA (1995) Formation of glasses from liquids and biopolymers. Science 267: 1924–1935

Arcangeli C, Bizzarri AR, Cannistraro S (1998) Role of interfacial water in the md simulated dynamical transition of plastocyanin. Chem Phys Lett 281: 7–14

Bèe M (1988) Quasielastic neutron scattering: principles and applications in solid-state chemistry, biology and material science. Hilger, Bristol

Bellissent-Funel MC, Teixeira J, Chen SH, Dorner B, Middendorf H, Crespi L (1989) Low-frequency collective modes in dry and hydrated proteins. Biophys J 56: 713–716

Berendsen HJC, Grigera JR, Straatsma TP (1987) The missing term in effective pair potentials. J Phys Chem 91: 6269–6271

Bizzarri AR, Cannistraro S (1996) Molecular dynamics simulation evidence of anomalous diffusion of protein hydration water. Phys Rev E 53: 3040–3043

Bizzarri AR, Rocchi C, Cannistraro S (1996) Origin of the anomalous diffusion observed by MD simulation at the protein-water interface. Chem Phys Lett 263: 559–566

Brown K, Erfurth S, Small EW, Peticolas WL (1972) Conformationally dependent low-frequency motions of proteins by laser raman spectroscopy. Proc Natl Accad Sci USA 69: 1467–1469

Buchenau U (1992) Soft localized vibrations in glasses and undercooled liquids. Philos Mag B 65: 303–315

Buchenau U, Wishnewski A, Richter D, Frick B (1996) Is the fast process at the glass transition mainly due to long wavelength excitations? Phys Rev Lett 77: 4035–4038

Chou KC (1985) Low-frequency motions in protein molecules. Biophys J 48: 289–297

Ciocchetti A, Bizzarri AR, Cannistraro S (1997) Long term MD simulation of copper plastocyanin in water. Biophys Chem 69: 185–198

Cusack S (1989) Low frequency dynamics of proteins: comparison of inelastic neutron scattering results with theory. Chem Scr 29A: 103–107

Cusack S, Doster W (1990) Temperature dependence of the low frequency dynamics of myoglobin. Biophys J 58: 243–251

Demmel F, Doster W, Petry W, Shulte A (1997) Vibrational frequency shifts as a probe of hydrogen bonds: thermal expansion and glass transition of myoglobin in mixed solvents. Eur Biophys J 26: 327–332

Diehl M, Doster W, Petry W, Schober H (1997) Water-coupled low frequency modes of myoglobin and lysozyme observed by inelastic neutron scattering. Biophys J 73: 2726–2730

Doster W, Bachleitner A, Dunau R, Hiebl M, Lusher E (1986) Thermal properties of water in myoglobin crystals and solutions at subzero temperatures. Biophys J 50: 213–219

Doster W, Cusack S, Petry W (1989) Dynamical transition of myoglobin revealed by inelastic neutron scattering. Nature 337: 754–756

Doster W, Cusack S, Petry W (1990) Dynamic instability of liquidlike motions in a globular protein observed by inelastic neutron scattering. Phys Rev Lett 65: 1080–1083

Elliott SR (1992) A unified model for the low-energy vibrational behaviour of amorphous solids. Europhys Lett 19: 201–206

Fan J, Cooper EI, Angell CA (1994) Glasses with strong calorimetric β-glass transitions and the relation to the protein glass transition problem. J Chem Phys 98: 9345–9349

Ferrand M, Dianoux AJ, Petry W, Zaccai G (1993) Thermal motions and function of bacteriorhodopsin in purple membranes: effects of temperature and hydration studied by neutron scattering. Proc Natl Acad Sci USA 90: 9668–9672

Fitter J, Lechner RE, Dencher NA (1997) Picosecond molecular motions in bacteriorhodopsin from neutron scattering. Biophys J 73: 2126–2137

Foley M, Wilson M, Madden PA (1995) Boson peaks and slow relaxation in a simulation of a network-forming ionic melt. Philos Mag B 71: 557–569

Frauenfelder H, Parak F, Young RD (1988) Conformational substates in proteins. Annu Rev Biophys Chem 17: 451–479

Frick B, Richter D (1993) Change of the vibrational dynamics near the glass transition in polyisobutylene: inelastic neutron scattering on a nonfragile polymer. Phys Rev B 47: 14795–14804

Frick B, Richter D (1995) The microscopic basis of the glass transition in polymers from neutron scattering studies. Science 267: 1939–1945

Genzel L, Keilmann F, Martin TP, Winterling G, Yacoby Y, Frölich H, Makinen MW (1976) Low frequency raman spectra of lysozyme. Biopolymers 15: 219–225

Go N (1978) Shape of the conformational energy surface near the global minimum and low-frequency vibrations in the native conformation of globular proteins. Biophys J 17: 1373–1379

Goetze W, Sjögren L (1992) Relaxation processes in supercooled liquids. Rep Prog Phys 55: 241–376

Green JL, Fan J, Angell CA (1994) The protein-glass analogy: some insights from homopeptide comparisons. J Phys Chem 98: 13780–13790

Gunsteren WF van, Berendsen HJC (1996) Groningen molecular simulation GROMOS, library manual. Biomos, Groningen

Iben IET, Braunstein D, Doster W, Frauenfelder H, Hong MK, Johnson JB, Luck S, Ormos P, Shulte A, Steinbach PJ, Xie AH, Young AD (1989) Glassy behaviour of a protein. Phys Rev Lett 62: 1916–1919

Kneller GR, Keiner V, Kneller M, Schiller M (1995) nMOLDYN: a program package for a neutron scattering oriented analysis of molecular dynamics simulations. Comput Phys Commun 91: 191–214

Levitt M, Sharon R (1988) Accurate simulation of protein dynamics in solution. Proc Natl Acad Sci USA 85: 7557–7561

Longarich RJ, Brooks BR (1990) Temperature dependence of dynamics of hydrated myoglobin: comparison of force field calculations with neutron scattering data. J Mol Biol 215: 439–455

Lounnas V, Petitt BM, Philips GN (1994) A global model of the protein-solvent interface. Biophys J 66: 601–614

Lovesey S (1986) Theory of neutron scattering from condensed matter. Oxford University Press, Oxford

Martel P, Calmettes P, Hennion B (1991) Vibrational modes of hemoglobin in red blood cells. Biophys J 59: 363–374

Melchionna S, Falconi M, Desideri S (1988) Effect of temperature and hydration on protein fluctuations: molecular dynamics simulation of Cu, Zn superoxide dismutase at six different temperatures: comparison with neutron scattering data. J Chem Phys 108: 1–9

Messing T, Growenborc B, Muller Hill B, Hofshneider DH (1977) Filamentous coliphage m13 as a cloning vehicle: insertion of hind in fragment of the lac regulatory region in m13 replicative firm in vitro. Proc Natl Acad Sci USA 74: 3642–3646

Middendorf HD (1984) Biophysical applications of quasi-elastic and inelastic neutron scattering. Rev Biophys Bioeng 13: 425–451

Nar H, Messerschmidt A, Huber R, van de Kamp M, Canters GW (1991) Crystal structure analysis of oxidized *Pseudomonas aeruginosa* azurin at pH 5.5 and pH 9.0. J Mol Biol 221: 765–772

Paciaroni A, Bizzarri AR, Cannistraro S (1998) Molecular-dynamics simulation evidences of a boson peak in protein hydration water. Phys Rev E 57: 6277–6280

Painter P, Mosher L, Rhoads C (1982) Low-frequency modes in the raman spectra of proteins. Biopolymers 21: 1469–1472

Parak F, Knapp EW (1984) A consistent picture of protein dynamics. Proc Natl Acad Sci USA 81: 7088–7092

Parak F, Knapp EW, Kucheida D (1982) Protein dynamics. Moessbauer spectroscopy on deoxymyoglobin crystals. J Mol Biol 161: 177–194

Rocchi C, Bizzarri AR, Cannistraro S (1998) Water dynamical anomalies evidenced by MD simulations at the solvent-protein interface. Phys Rev E 57: 3515–3522

Ryckaert JP, Ciccotti G, Berendsen HJC (1977) Numerical integration of the cartesian equations of motions of a system. J Comput Phys 23: 327–333

Settles M, Doster W (1996) Anomalous diffusion of adsorbed water: a neutron scattering study of hydrated myoglobin. Faraday Discuss Chem Soc 103: 269–279

Smith J (1991) Protein dynamics: comparison of simulations with inelastic neutron scattering experiments. Q Rev Biophys 24: 227–291

Smith J, Kuczera K, Tidor B, Doster W, Cusack S, Karplus M (1989) Internal dynamics of globular proteins: comparison of neutron scattering measurements and theoretical models. Physica B 156–157: 437–443

Smith J, Kuczera K, Karplus M (1990) Dynamics of myoglobin: comparison of simulation results with neutron scattering spectra. Proc Natl Acad Sci USA 87: 1601–1605

Smith JC, Kneller GR (1993) Combination of neutron scattering and molecular dynamics to determine internal motions in biomolecules. Mol Simul 10: 363–375

Sokolov AP, Kisliuk A, Soltwish M, Quitmann D (1992) Medium-range order in glasses: comparison of Raman and diffraction measurements. Phys Rev Lett 69: 1540–1543

Steinbach PJ, Brooks BR (1996) Hydrated myoglobin's anharmonic fluctuations are not primarily due to dihedral transitions. Proc Natl Acad Sci USA 93: 55–59

Steinbach PJ, Loncharich RJ, Brooks BR (1991) The effects of environment and hydration on protein dynamics: a simulation study of myoglobin. Chem Phys 158: 383–394

Ungar LW, Scherer NF, Voth GA (1997) Classical molecular dynamics simulation of the photoinduced electron transfer dynamics of plastocyanin. Biophys J 72: 5–17

Wuttke J, Petry W, Coddens G, Fujara F (1995) Fast dynamics of glass-forming glycerol. Phys Rev E 52: 4026–4034

Zeller C, Pohl RO (1971) Thermal conductivity and specific heat of non-crystalline solids. Phys Rev B 4: 2029–2041